AJRCCM Articles in Press. Published on September 24, 2009 as doi:10.1164/rccm.200906-0892OC

Toll-like Receptor 9 Activation is a Key Mechanism for the Maintenance of Chronic Lung Inflammation

Toshihiro Ito,[1] Matthew Schaller,[1] Tracy Raymond,[1] Amrita D. Joshi,[1] Ana L. Coelho,[1] Fabiani G. Frantz,[1] William F. Carson IV,[1] Cory M. Hogaboam,[1] Nicholas W. Lukacs,[1] Theodore J. Standiford,[2] Sem H. Phan,[1] Stephen W. Chensue,[1,3] and Steven L. Kunkel[1]

[1]Department of Pathology, University of Michigan Medical School, Ann Arbor, MI 48109-2200, USA
[2]Division of Pulmonary and Critical Care Medicine, Department of Medicine, University of Michigan Medical Center, Ann Arbor, MI 48109, USA
[3]Department of Pathology and Laboratory Medicine, Veterans Affairs Ann Arbor Healthcare System, Ann Arbor, MI 48105, USA

Contact: Steven L. Kunkel, Ph.D.
Immunology Program, Department of Pathology, University of Michigan Medical School
4071 BSRB, 109 Zina Pitcher Place, Ann Arbor, MI 48109-2200, USA
E-mail: slkunkel@umich.edu, Fax: +1-734-764-2397, Phone: +1-734-936-1020

Supported by NIH (National Institutes of Health) grants P01-HL031963, HL092853, HL089216, and HL031237.

Conflict of interest statement: None of the authors has a financial relationship with a commercial entity that has an interest in the subject of this manuscript.

Running title: TLR9 in Type-2 Pulmonary Granuloma

Descriptor number: 82. Pathology of immunologic and interstitial lung disease

Word Count for the body of the manuscript: 5276 words

AT A GLANCE COMMENTARY

Scientific Knowledge on the Subject

A number of studies have suggested that the innate immune response not only supports acute inflammation, but also provides a bridge into the maintenance of the chronic inflammatory response. However, the mechanistic role of the innate immune response to the development of antigen-dependent chronic lung inflammation has not been well studied.

What This Study Adds to the Field

We demonstrate that the initiation and maintenance of chronic lung inflammation induced in Toll-like receptor 9 (TLR9)-knockout mice is associated with an augmented granulomatous lung response, increased collagen deposition, skewed Th2 cytokine phenotype, impaired DC function, and activation of alternatively-activated macrophages characterized by the production of "found in inflammatory zone-1" (FIZZ1).

This article has an online data supplement, which is accessible from this issue's table of content online at www.atsjournals.org

ABSTRACT

Rationale: Accumulating evidence supports the hypothesis that the continuous host response to a persistent challenge can polarize the cytokine environment toward a Th2 cytokine phenotype, but the mechanisms responsible for this skewing is not clear.

Objectives: We investigated the role of Toll-like receptor 9 (TLR9) in a Th2-driven pulmonary granulomatous response, initiated via the embolization of *Schistosoma mansoni* eggs to the lungs of mice.

Methods: Mice were intravenously injected with *Schistosoma mansoni* eggs. Histological and flow cytometric analysis, cytokine measurement, adoptive transfer of bone marrow (BM)-derived dendritic cells (DCs), and *in vitro* T cell treatments with antigen-presenting cells (APCs) were examined.

Measurements and Main Results: In comparison to WT mice, $TLR9^{-/-}$ mice showed an increase in pulmonary granuloma size, augmented collagen deposition, an increase in the Th2 cytokine phenotype, impaired accumulation of DCs. BM-derived DCs, but not macrophages, recovered from animals with developed Th2-type lung granulomas promoted the production of type 2 cytokines from $CD4^+$ T cells. Furthermore, BM-derived DCs from $TLR9^{-/-}$ mice induced impaired Th1 cytokine and enhanced Th2 cytokine production by T cells, compared with DCs from WT mice. Macrophages from $TLR9^{-/-}$ mice expressed a significantly higher alternatively activated (M2) phenotype characterized by increased "found in inflammatory zone-1" (FIZZ1) and Arginase-1 expression. The adoptive transfer of BM-derived DCs from syngeneic WT mice into $TLR9^{-/-}$ mice, restored the granuloma phenotype seen in WT mice.

Conclusions: These studies suggest that TLR9 plays an important mechanistic role in the

maintenance of the pulmonary granulomatous response.

Word Count for the Abstract: 245 words

Key Words: granuloma; pulmonary fibrosis; innate immunity; dendritic cell; macrophage

INTRODUCTION

The granulomatous response is a complex host defense mechanism that has evolved to provide containment of infectious and/or environmental agents (1, 2). Although this reaction is designed to be protective, the associated tissue injury is often responsible for a profound degree of pathology. While many of the mechanisms that sustain the development of the granuloma are enigmatic, it is accepted that the maintenance of this inflammatory process are dependent upon dynamic interactions between an inciting agent, inflammatory mediators, various immune and inflammatory cells, and structural cells of the involved tissue (3). The best studied of the host-dependent processes during granuloma development is the adaptive immune response, which is characterized by specific immune cell populations expressing a defining phenotype of inflammatory mediators (3-8). Recent data also suggests that the innate immune response initiated by the activation of specific toll-like receptors can mechanistically contribute to maintaining the intensity and chronicity of the lung pathology associated with the developing granuloma (9-11).

We have utilized an experimental system of granuloma development via the embolization of *schistosoma mansoni* eggs to the lungs, which release highly antigenic glycoproteins, referred to as Schistosoma egg antigen (SEA) that promote a dominant Th2 responses (11). In its chronic phase, this inflammatory response promotes a dominant Th2 cytokine-driven response characterized by IL-4, IL-5, and IL-13, which involves the recruitment and activation of eosinophils, alternatively activated (M2) macrophages, dendritic cells (DCs), $CD4^+$ Th2 cells, and the development of fibrotic granulomas (12, 13). While a significant body of data exists on the cytokine phenotype

and cellular composition of developing lung granulomas, little is know about the mechanistic contribution of TLRs to the maintenance and fibrotic aspect of this inflammatory response.

In the present study, we investigated the contribution of TLR9 to the initiation and maintenance of a Th2-dependent lung granulomatous response. We demonstrate that TLR9-deficient mice develop significantly larger granulomas with augmented collagen deposition, associated with a selective abrogation in IFN-γ (Th1 cytokine) production, enhanced Th2 (IL-4, IL-5, and IL-13) cytokine profile, and an increased M2 macrophage phenotype (FIZZ1 and Arginase-1) in the lung. Interestingly, our *in vivo* experiments demonstrate functional relevance for FIZZ1, as the intranasal administration of recombinant FIZZ1 enhanced collagen deposition in the Th2-dependent lung granulomas. We also found that antigen-pulsed BM-derived DCs, but not BM-derived macrophages, both from naïve mice, promoted both Th1 and Th2 effector activation of $CD4^+$ T cells. Our results further show that the adoptive transfer of BM-derived DCs isolated from WT mice, but not from $TLR9^{-/-}$ mice, can restore the granulomatous response in $TLR9^{-/-}$ to a WT phenotype. Taken together, our results indicate that TLR9 plays a key role in the initiation and maintenance of Th2 type-pulmonary granulomatous inflammation.

METHODS

Mice

Male WT mice and male DO11.10 mice, both on a BALB/c background, were purchased from The Jackson Laboratories (Bar Harbor, ME). Male BALB/c mice lacking the TLR9 gene ($TLR9^{-/-}$) were provided by T. J. Standiford. All mice were used for experiments at 8-12 week of age. These mice were maintained under specific pathogen-free conditions and provided with food and water ad libitum in the University Laboratory Animal Medicine (ULAM) facility at the University of Michigan Medical School. All animal protocols were approved by ULAM.

Antibodies

Rat mAbs specific for mouse CD11b (M1/70), CD11c (HL3), CD16/32 (2.4G2), CD45 (30-F11), and CD45R/B220 (RA3-6B2) were purchased from BD PharMingen (San Diego, CA). Rat Anti-F4/80 (CI: A3-1) mAb was purchased from Serotec (Raleigh, CA).

Th2-driven lung granuloma model

Mice were intravenously injected with 5000 viable *S. mansoni* eggs via the tail vein. Live *S. mansoni* eggs were purified from the livers of *S. mansoni* cercariae-infected Swiss-Webster mice, which were kindly provided by Dr. Fred Lewis (Biomedical Research Laboratory, Rockville, MD). Mice were sacrificed 4, 8, 16, or 30 days after intravenous injection. In some experiments, mice were treated with 5 μg recombinant FIZZ-1 (Peprotech Inc., Rocky Hill, NJ) or PBS intranasally on days 9, 11, 13, 15 of egg challenge, and sacrificed on day 16.

Histological and Immunofluorescent examination

Individual excised lung lobes were inflated and fixed with 10% buffered formalin for morphometric analysis. The areas of the granulomas were measured in a blinded fashion on H&E-stained sections of paraffin-embedded lungs using IP Lab Spectrum software, and morphometric analysis of collagen present in Masson's Trichrome-stained lung sections was also carried out using light microscopy and the same software as described previously (11). For immunofluorescent analysis, lungs were embedded in Tissue-Tek OCT compound (Sakura Finetek, Torrance, CA), and then frozen in liquid nitrogen. Seven-micron cryostat sections were fixed in ice-cold acetone, then incubated with primary antibodies, followed by appropriate Alexa-labeled secondary reagents (Invitrogen Corporation, Garlsbad, CA). Finally, the sections were analyzed by Zeiss LSM 510 confocal microscope system (Carl Zeiss Inc., Thornwood, NY).

Reverse Transcription and Real-time Quantitative PCR Analysis

Total RNA was isolated from whole lungs or cultured cells by using TRIzol (Invitrogen) according to manufacturer's instructions. Briefly, a total of 2.0 μg of RNA was reverse-transcribed to cDNA, and real-time quantitative PCR analysis was performed by using ABI 7700 sequence detector system (PE Applied Biosystems, Foster City, CA).

Protein analysis of cytokine

Murine cytokine levels were measured in 50 μl samples from whole lung homogenates using a Bio-plex bead-based cytokine assay purchased from Bio-Rad Laboratories

(Hercules, CA). FIZZ1 protein levels were measured by ELISA as described before (10). The cytokine levels in lung homogenates were normalized to the protein (in milligrams) using the Bradford assay. Cells were plated at a concentration of 5 x 10^6/ml onto a 96 well plate, and then re-stimulated with purified SEA at 10 μg/ml. Supernatants were harvested 48 hours after stimulation and analyzed by Bio-plex assay.

Flow Cytometry

Flow cytometric analyses of lung cells were performed as previously described (14). Briefly, whole lungs were dispersed in RPMI1640 containing 0.2% collagenase (Sigma-Aldrich, St. Louis, MO) and 5% fetal bovine (Atlas, Fort Collins, CO) serum at 37°C for 45min to obtain a single-cell suspension. The cells were stained with indicated antibodies after 10 min of pre-incubation with CD16/CD32 Abs (Fc block), and fixed overnight with 4% formalin. Cells were analyzed using a Cytomics FC-500 (Beckman Coulter, Miami, FL) and data were analyzed by FlowJo software (TreeStar, Inc., Ashland, OR).

Generation of BM-derived DCs

For generation of BM-derived DCs, after depletion of erythrocytes with lysis buffer, BM cells were seeded in T-150 tissue culture flasks at 10^6 cells/ml in RPMI 1640-based complete media with GM-CSF 20 ng/ml (R&D Systems, Minneapolis, MN). 6 days later, loosely adherent cells were collected and incubated with anti-CD11c coupled to magnetic beads for positive selection of conventional DCs from the GM-CSF cultures using a magnetic column (>95% purity) (Miltenyi Biotec, Auburn, CA). For generation of BM-derived macrophages, BM cells were cultured in L929 cell-conditioned medium as

described previously (14). In some experiments, after 2 hours stimulation with SEA (10 μg/ml) at 37℃ and 5% CO_2, BM-derived DCs were administered intratracheally into mice.

In vitro T cell treatments

BM-derived DCs or macrophages were plated on 96-well plates at a cell density of 4 x 10^4 cells/well and incubated overnight. DCs or macrophages were then pulsed with SEA (10 μg/ml) for 2 hours, and washed before adding T cells. 16 days after intravenous injection of 5000 *S. mansoni* eggs, $CD4^+$ T cells from lungs, draining lymph nodes, or spleens were isolated using a magnetic bead column (>95% purity). These cells (2 x 10^5 cells/well) were exposed to SEA-pulsed BM-derived DCs or macrophages on 96-well plates at APC:$CD4^+$ cell ratio of 1:5 (lungs), or of 1:20 (draining lymph nodes and spleens). Supernatants were harvested 48 hours later for analysis in a Bio-plex bead-based cytokine assay.

Statistical analysis

Two-tailed Student's t test was used to compare groups. Values of $P < 0.05$ were considered significant.

RESULTS

The chronicity of the pulmonary granulomatous response is augmented in $TLR9^{-/-}$ mice

Recent data suggests that mechanisms that drive the innate immune response, such as activation of the TLR system, serves as a novel bridge to facilitate the acquired immune response (14, 15). To further explore this notion, we determined whether TLR9 is involved in the development of the Th2-type pulmonary granulomatous response. Initially we examined histological lung sections from WT and TLR9$^{-/-}$ mice at days 4, 8, 16, and 30 after initiation of the primary Th2 response. Histological examination of lung tissue revealed that the granulomas were similar in size in both WT and TLR9$^{-/-}$ mice for the first 4 days after challenge (Figure 1A). However, at day 8 Masson's Trichrome stained lung sections revealed that TLR9$^{-/-}$ mice exhibited significantly larger granulomas, as determined by morphometric analysis when compared with WT mice (Figure 1B). Associated with the enhanced granuloma size is the appearance of a significant amount of matrix deposition starting at day16 in the TLR9$^{-/-}$ mice (Figure 1C). There are neither pathologic nor abnormal features in naïve TLR9$^{-/-}$ mice; their lung tissues appear normal. In addition, granulomatous lungs of TLR9$^{-/-}$ mice expressed significantly higher levels of α-SMA mRNA expression (Figure 1D), as compard to WT mice. These results were further supported by confocal immunofluorescent analysis, which showed an increase in α-SMA^{+} cells (green) associated with the local granuloma in TLR9$^{-/-}$ mice (Figure 1E).

Lungs from TLR9$^{-/-}$ mice demonstrate increased Th2 and decreased Th1 cytokines during pulmonary granuloma formation

To help elucidate the mechanism underlying the changes in pulmonary granuloma size and collagen deposition in TLR9$^{-/-}$ mice versus WT mice, we examined the cytokine

profile in the granulomatous lungs. Whole lungs from TLR9$^{-/-}$ mice had significantly lower protein levels of Th1 dependent cytokines, such as IFN-γ and IL-12p70, and TNF-α, while protein levels of cytokines that promote the Th-2 biased immune response (*i.e.*, IL-4, IL-5, and IL-13) were significantly increased in TLR9$^{-/-}$ mice, as compared to WT mice (Figure 2A). Further mRNA analysis also confirmed lower expression of Th1 type cytokines (*i.e.*, IFN-γ, IL-12p35, and TNF-α) (Supplemental Figure 1). IL-12p40 mRNA expression was below detection levels of our assay (data not shown). We also characterized the production of Th1 and Th2 cytokines from cells recovered from draining lymph nodes of granulomatous mice after in vitro rechallenge with SEA. The data illustrate that there were considerable decreases in IFN-γ production from the lymph node derived cells from the TLR9$^{-/-}$ mice compared with WT mice, while the Th2 cytokines IL-4, -5, and -13 were significantly up-regulated in TLR9$^{-/-}$ mice compared with WT mice (Figure 2B).

We also evaluated M1 and M2 macrophage markers in the developing granulomas from WT and TLR9$^{-/-}$ mice. The expression level of M2 markers FIZZ1 (both mRNA and protein) (Figure 3A and 3B) and Arginase-1 (mRNA) (Figure 3C) were significantly increased in TLR9$^{-/-}$ mice compared with WT mice. In contrast, iNOS, a M1 macrophage marker, was significantly less in TLR9$^{-/-}$ mice at day 16 and 30 (Figure 3D).

Granulomaotus lungs from TLR9$^{-/-}$ mice display reduced numbers of DCs and increased number of macrophages

To further characterize the changes in cell phenotype between WT and TLR9$^{-/-}$ mice during granuloma formation, we assessed the numbers of antigen presenting cells

(APCs) in granulomatous lungs by examining $CD45^+$ leukocytes. Compared with WT mice, the number of myeloid DCs (mDCs) ($CD11b^+CD11c^+$) was significantly decreased in $TLR9^{-/-}$ mice at Day 16 (Figure 4A). There was no significant difference in the number of plasmacytoid DCs (pDCs) ($B220^+CD11c^+$) (data not shown). In contrast, the number of $F4/80^+$ macrophages was significantly increased in $TLR9^{-/-}$ mice at Day 16 (Figure 4B). These results were also supported by confocal immunofluorescent analysis, which showed fewer $CD11c^+$ staining cells (red) and an increase in $F4/80^+$ cells (green) associated with the local lung granulomas in $TLR9^{-/-}$ mice (Figure 4C). To further determine the reason why the number of DCs was reduced in $TLR9^{-/-}$ mice, we investigated chemokine expression during granuloma formation. As shown in Figure 4D, the mRNA expression levels of CCL20 and CCL22 were significantly decreased in $TLR9^{-/-}$ mice. Interestingly, these chemokines have been shown to play a crucial role in the recruitment of immature DCs into inflammatory lesions (16, 17). Moreover, the mRNA expression levels of CXCL9, CXCL10, and CXCL11, which support the migration of Th1 cells (18), were significantly reduced in $TLR9^{-/-}$ mice. In contrast, the expression level of CCL17, which is released from M2 macrophages and supports the migration of Th2 cells (19), was significantly increased in $TLR9^{-/-}$ mice.

BM-derived DCs but not macrophages promote the expression of Th1 and Th2 cytokines from T cells during a Th2-induced immune response

Since there is significant difference in Th1/Th2 cytokine balance between WT and $TLR9^{-/-}$ mice during pulmonary granuloma formation, we next assessed whether

these APCs (DCs and macrophages) could promote $CD4^+$ T effector cell expression upon pulsing with SEA using a co-culture cytokine elicitation assay. As shown in Figure 5, DCs, but not macrophages, were capable of inducing Th1 cytokine (IFN-γ) and Th2 cytokines (IL-4, IL-5, and IL-13) expression from the $CD4^+$ cells. Interestingly, IFN-γ production was significantly less when the DCs were derived from $TLR9^{-/-}$ mice, while IL-4, IL-5, and IL-13 production was significantly increased using DCs recovered from $TLR9^{-/-}$ mice.

BM-derived DCs from mice with *S. mansoni* egg-induced granulomas induce enhanced Th2-shifted response from lung $CD4^+$ T cells

To further investigate whether the Th2 cyokine polarization evoked by *S. mansoni* eggs was successfully supported by DCs, we performed an *in vitro* cytokine expression assay using lung $CD4^+$ T cell, recovered from granulomatous lungs, co-incubated with SEA-pulsed BM-derived DCs from either WT or $TLR9^{-/-}$ mice recovered from either naïve or granulomatous mice. In the presence of DCs derived from mice with pulmonary granulomas, lung $CD4^+$ T cells (also from granulomatous lungs) demonstrated reduced IFN-γ production and increased IL-4, IL-5, and IL-13 production (Figure 6). Additionally, the APC function of DCs from the $TLR9^{-/-}$ mice, as compared to WT DC, caused a decrease in Th1 cytokine (IFN-γ) production and an increase in Th2 cytokine (IL-4, IL-5, and IL-13) production. These responses were also seen when using $CD4^+$ T cells from draining lymph nodes (Supplemental Figure 2). To determine whether these responses were antigen specific, we evaluated the production of the above cytokines by splenic

$CD4^+$ T cells from DO11.10 mice, which have an OVA-specific TCR. These cells were co-cultured with BM-derived DCs from WT or $TLR9^{-/-}$ mice recovered from either mice with developing Th2 lung granulomas or from naïve mice. No significant differences in the production of Th1 and Th2 cytokines were seen in T cells co-cultured with BM-derived DCs under any of the described experimental conditions after stimulation with only OVA peptide (Supplemental Figure 3). These results underscore the specificity of the response to the original sensitizing antigen, SEA, as well as the importance of DC-derived TLR9 activation in eliciting the Th1 phenotype during T cell activation events.

Reconstitution of the wild type pulmonary granulomatous response in $TLR9^{-/-}$ mice after adoptive transfer of WT syngenetic BM-derived DCs

Studies contained in this manuscript have demonstrated an impairment of DC accumulation and effector cell function in $TLR9^{-/-}$ mice after *S. mansoni* egg challenge. To determine whether these DC defects contributed meaningfully to larger granuloma and impaired cytokine balance during pulmonary granuloma formation in TLR9-deficient mice, we adoptively transferred BM-derived DC recovered from WT mice into $TLR9^{-/-}$ mice and then assessed histological appearance and cytokine production. For these experiments, we administrated BM-derived DCs intratracheally, an approach that has previously been shown to stimulate intrapulmonary immunity in other model systems in which the inflammatory response was localized to the lung (20). BM-derived DCs (1×10^6 cells) obtained from WT mice or $TLR9^{-/-}$ mice were administered i.t. just after *S. mansoni* egg challenge. Lungs were harvested 16 days later and histological assessment

was determined. As shown in Figure 7, granulomatous lungs administrated BM-derived DCs from WT mice histologically and morphometrically demonstrated a reduced granuloma size (Figure 7A and 7B) and a reduction in collagen deposition (Figure 7C), compared with those animals receiving BM-derived DCs from TLR9$^{-/-}$ mice. In addition, the intratracheal delivery of WT DC into TLR9$^{-/-}$ mice resulted in a marked reduction in Th2 cytokines (IL-4, IL-5, and IL-13) production (Figure 8 A-C), while these difference were not seen when TLR9$^{-/-}$-DC are administrated. Moreover, the production of Th1 and Th2 cytokines from draining lymph nodes of treated mice was assessed after in vitro re-challenge with SEA. There was a significant increase in IFN-γ production (Supplemental Figure 4A), while the Th2 cytokines, IL-4 and IL-5, were significantly decreased in the lymph nodes of mice that received DCs isolated from WT mice compared with mice given DCs from TLR9$^{-/-}$ mice (Supplemental Figure 4B and 4C). There were no significant differences in the production of IL-13 between these two groups, though these levels were significantly reduced compared with the control (PBS) group (Supplemental Figure 4D). In addition, the protein level of FIZZ1 (Figure 8D) in whole lungs was significantly decreased after i.t. transfer of WT DC, but not in lungs of mice given DC from TLR9$^{-/-}$ mice.

Intranasal administration of recombinant FIZZ1 enhanced collagen deposition during granuloma formation in both WT and TLR9$^{-/-}$ mice

FIZZ1 plays an important role in the fibrotic response, and lungs from TLR9$^{-/-}$ deficient mice with a developing Th2-dependent pulmonary granuloma displayed enhanced FIZZ1 expression. To further investigate the distinct role of FIZZ1 in vivo, we performed intranasal administration of recombinant FIZZ1 into both WT and TLR9$^{-/-}$

mice during granuloma formation. Histologic and collagen analysis demonstrated that exogenous treatment with recombinant FIZZ1 in both WT and TLR9$^{-/-}$ mice significantly enhanced collagen deposition (Figure 9A and B). Further investigations showed that there were no significant difference in granuloma size and the Th1 and Th2 cytokine profile in the granulomatous lungs demonstrated no significant difference between PBS- and recombinant FIZZ1-treated group (data not shown).

DISCUSSION

Our results demonstrate that the TLR9 signaling pathway is essential in the regulation of an antigen dependent, Th2 cytokine driven granulomatous response. To our knowledge, the present investigation represents the first analysis of cell-mediated Th2 pulmonary granuloma formation in mice with targeted disruption of the TLR9 gene. Our studies demonstrate that the developing granulomatous response in the TLR9-deficient mice exhibit a significantly larger granuloma, augmented type 2 cyokine expression, and a higher collagen content. The altered histological findings in TLR9$^{-/-}$ mice coincided with significantly decreased whole-lung IFN-γ, IL-12 and TNF-α levels and significantly increased whole-lung levels of IL-4, IL-5, and IL-13 during the formation and maintenance of the granuloma responses when compared with WT mice.

While TLR are known to provide the link between the innate and adaptive immunity (15), the relative contribution of each TLR to this process remains poorly described. The immune system can discriminate between different microbes through

various pathogen-recognition receptors, such as TLRs, members, which are highly evolutionarily conserved (21, 22). Upon antigenic stimulation by APCs, naïve $CD4^+$ T cells become activated, expand, and differentiated into various effector T cell helper subsets termed Th1 and Th2, and characterized by the production of distinct cytokines and effector functions (23, 24). TLR signaling has been considered to be important in the pathogenesis of pulmonary inflammatory diseases such as lung fibrosis and bronchial asthma (25). Specifically, TLR4- and TLR5-mediated innate immunity plays an important role in cystic fibrosis lung disease (26, 27), and respiratory viral infection (28). In this latter study, the recruitment of Th2 cytokine-producing cells may amplify Th2-dependent inflammation via the induction of TLR3 in the asthmatic airway (28). Furthermore, we have also demonstrated that TLR3 regulates the immunopathology associated with the Th2-type pulmonary granulomatous response (11). Previous studies have also shown that clinical helminth infections are associated with profound alterations in the expression and activation of various TLR on immune cells; For example, SEA directly inhibits the ability of DC to respond to LPS (a TLR4 ligand) and CpG (a TLR9 ligand) (29, 30). In this study we showed that SEA-pulsed DCs, but not macrophages, supported Th1/Th2 cytokine production by $CD4^+$ T cells after re-stimulation. We further established that the adoptive transfer of BM-derived WT-DC, but not BM-derived DC from $TLR9^{-/-}$ mice, administered directly into the lung, markedly recapitulated the granuloma phenotype in WT mice with reduced Th2 cytokine production. In addition, $TLR9^{-/-}$ mice did not show an alteration in other TLRs that could account for the differences seen in the development of Th2-type pulmonary granulomatous response (data not shown). Together, our results provide evidence of defective DC responses in

TLR9$^{-/-}$ mice. Currently the potential therapeutic effect of unmethylated CpG DNA for experimental chronic lung disease is under investigation in our laboratory. Further studies are in progress to assess the potential role of other TLRs in the development of the Th2-type granulomatous response in the progression of inflammatory airway disease and exacerbation of pulmonary fibrosis.

Further evidence of a strongly skewed Th2 response in the granulomas developing in the TLR9$^{-/-}$ mice was the presence of M2 macrophages. They express unique markers such as FIZZ1, which are not expressed by M1 macrophages (31). It has been proposed that the *in vivo* induction of FIZZ1 in macrophages depends on IL-4 (32). Additionally, arginase production is significantly increased in M2-polarized macrophages. This enzyme blocks iNOS activity by a variety of mechanisms, including competing for the arginase substrate that is required for NO production and needed for the successful killing of invading pathogens (33). We have demonstrated in this study that the lungs of TLR9$^{-/-}$ mice showed decreased iNOS expression and increased expression of FIZZ1 and Arginase-1; characteristic of M2 skewing. FIZZ1 directly induces fibroblast differentiation and increases expression of α-SMA, and also has an anti-apoptotic effect on mouse lung fibroblasts, which can impact the survival of the myofibroblast in the context of the pulmonary fibrotic response (32, 34, 35). Our data establish that FIZZ1 is an important molecule during the development of a Th2-dependent pulmonary granuloma. Recent evidence suggests that *in vivo* gene transfer of FIZZ1 in the chronic hypoxia model of pulmonary hypertension enhanced the vascular remodeling including thickening and muscularization of small arterioles (36). This report agrees with our findings showing that FIZZ1 administration *in vivo* during the initiation of the Th2

granuloma significantly increases collagen deposition. Determining the mechanism may revel a potential clinical target for granuloma disease as well as for pulmonary hypertension.

A number of studies have shown that TGFβ promotes collagen synthesis, fibroblast proliferation and transdifferentiation into myofibroblasts (37, 38). In our Th2 driven granuloma model, there is no significant difference in TGFβ levels between WT and TLR9$^{-/-}$ mice (data not shown). IL-13 can stimulate fibroblast collagen production independently of TGFβ (39, 40), and can also stimulate production of FIZZ1 (32). So we believe that enhanced collagen deposition in TLR9$^{-/-}$ mice is TGFβ independent, while IL-13 is a key cytokine in this experimental system that contributes to the fibrotic changes found in the developing granulomas.

Chemokines constitute a family of structurally related chemotactic cytokines that direct the migration of leukocytes throughout the body under both physiological and inflammatory conditions (41). CCL20 and CCL22 play a role in the recruitment of immature DCs and their precursors to sites of potential antigen entry (16, 17). The lower expression of CCL20 and CCL22 during granuloma development in TLR9-deficient lungs may contribute to the decreased DC numbers observed during pulmonary granuloma formation. In addition, lungs from TLR9$^{-/-}$ mice were found to express lower levels of CXCL9, CXCL10, and CXCL11, which are all ligands for CXCR3 on Th1 cells (18). These chemokine-related data might explain the impaired DC migration and decreased Th1 cytokine production in TLR9-deficient lungs during the evolution of the Th2 dependent pulmonary granuloma. Using confocal laser microscopy, we demonstrated a larger difference in DC and macrophage populations in the granulomas. However, the

percentage difference of DC and macrophage in our flow data using whole lung tissue appears small, which may be due to the fact that the confocal data used intact lung lesions and the flow data used entire lung tissue.

CXCL10 has been shown to be produced by M1 macrophages, while CCL17 has been shown to be produced by M2 macrophages (42). CCL17 is an effector molecule that inhibits M1 macrophage generation as well as Th1 cytokine (IFN-γ) production (19). The above published reports agree with our findings, which show that CCL17 expression was enhanced in TLR9$^{-/-}$ mice compared with WT mice, as the Th2 granuloma develops.

In summary, we present a comprehensive *in vivo* analysis of TLR9 participation in a granuloma model induced by Th2 skewing antigens. TLR9 deficiency resulted in an accelerated granulomatous response, a decreased Th1 and an increased Th2 cytokine profile during pulmonary granuloma formation. This increased Th2 cytokine environment induced a M2 macrophage phenotype characterized by the over-expression of FIZZ1, an M2 marker protein. FIZZ1 was demonstrated to possess an important function, as the administration of recombinant FIZZ1 *in vivo* induced enhanced collagen deposition in granulomas developing in both TLR9$^{-/-}$ and WT mice. Furthermore, the transfer of WT BM-derived DCs inhibited much of the augmented inflammatory response during granuloma formation in the TLR9$^{-/-}$ mice. This study supports the concept that a more clear understanding of chronic lung inflammation maintained by a Th2 response may provide mechanistic information to support a strategy to treat a number of enigmatic chronic lung diseases.

Acknowledgements

This work was supported by NIH (National Institutes of Health) grants P01-HL031963, HL092853, HL089216, and HL031237. We also thank Robin Kunkel, Ron Allen, Pam Lincoln, and Holly Evanoff for their technical assistance, as well as Dr. Judith Connett for her critical reading of the manuscript.

References

(1) Boros DL. Granulomatous inflammations. *Prog Allergy* 1978;24:183-267.

(2) El-Zammar OA, Katzenstein AL. Pathological diagnosis of granulomatous lung disease: a review. *Histopathology* 2007;50:289-310.

(3) Ulrichs T, Kaufmann SH. New insights into the function of granulomas in human tuberculosis. *J Pathol* 2006;208:261-269.

(4) Chensue SW, Ruth JH, Warmington K, Lincoln P, Kunkel SL. In vivo regulation of macrophage IL-12 production during type 1 and type 2 cytokine-mediated granuloma formation. *J Immunol* 1995;155:3546-3551.

(5) Ruth JH, Warmington KS, Shang X, Lincoln P, Evanoff H, Kunkel SL, Chensue SW. Interleukin 4 and 13 participation in mycobacterial (type-1) and schistosomal (type-2) antigen-elicited pulmonary granuloma formation: multiparameter analysis of cellular recruitment, chemokine expression and cytokine networks. *Cytokine* 2000;12:432-444.

(6) Qiu B, Frait KA, Reich F, Komuniecki E, Chensue SW. Chemokine expression dynamics in mycobacterial (type-1) and schistosomal (type-2) antigen-elicited pulmonary granuloma formation. Am J Pathol 2001;158:1503-1515.

(7) Chiu BC, Freeman CM, Stolberg VR, Komuniecki E, Lincoln PM, Kunkel SL, Chensue SW. Cytokine-chemokine networks in experimental mycobacterial and schistosomal pulmonary granuloma formation. *Am J Respir Cell Mol Biol* 2003;29:106-116.

(8) Chiu BC, Freeman CM, Stolberg VR, Hu JS, Komuniecki E, Chensue SW. The innate pulmonary granuloma: characterization and demonstration of dendritic

cell recruitment and function. *Am J Pathol* 2004;164:1021-1030.

(9) Fenhalls G, Squires GR, Stevens-Muller L, Bezuidenhout J, Amphlett G, Duncan K, Lukey PT. Associations between toll-like receptors and interleukin-4 in the lungs of patients with tuberculosis. *Am J Respir Cell Mol Biol* 2003;29:28-38.

(10) Ito T, Schaller M, Hogaboam CM, Standiford TJ, Chensue SW, Kunkel SL. TLR9 activation is a key event for the maintenance of a mycobacterial antigen-elicited pulmonary granulomatous response. *Eur J Immunol* 2007;37:2847-2855.

(11) Joshi AD, Schaller MA, Lukacs NW, Kunkel SL, Hogaboam CM. TLR3 modulates immunopathology during a Schistosoma mansoni egg-driven Th2 response in the lung. *Eur J Immunol.* 2008;38:3436-3449.

(12) Pearce EJ, MacDonald AS. The immunobiology of schistosomiasis. *Nat Rev Immunol* 2002;2:499-511.

(13) Herbert DR, Hölscher C, Mohrs M, Arendse B, Schwegmann A, Radwanska M, Leeto M, Kirsch R, Hall P, Mossmann H, Claussen B, Förster I, Brombacher F. Alternative macrophage activation is essential for survival during schistosomiasis and downmodulates T helper 1 responses and immunopathology. *Immunity* 2004;20:623-635.

(14) Ito T, Schaller M, Hogaboam CM, Standiford TJ, Sandor M, Lukacs NW, Chensue SW, Kunkel SL. TLR9 regulates the mycobacteria-elicited pulmonary granulomatous immune response in mice through DC-derived Notch ligand delta-like 4. *J Clin Invest* 2009;119:33-46.

(15) Akira S. Mammalian Toll-like receptors. *Curr Opin Immunol* 2003;15:5-11.

(16) Schutyser E, Struyf S, Van Damme J. The CC chemokine CCL20 and its receptor

CCR6. *Cytokine Growth Factor Rev* 2003;14:409-426.

(17) Hirota K, Yoshitomi H, Hashimoto M, Maeda S, Teradaira S, Sugimoto N, Yamaguchi T, Nomura T, Ito H, Nakamura T, Sakaguchi N, Sakaguchi S. Preferential recruitment of CCR6-expressing Th17 cells to inflamed joints via CCL20 in rheumatoid arthritis and its animal model. *J Exp Med* 2007;204:2925-2934.

(18) Liu L, Callahan MK, Huang D, Ransohoff RM. Chemokine receptor CXCR3: an unexpected enigma. *Curr Top Dev Biol* 2005;68:149-81.

(19) Katakura T, Miyazaki M, Kobayashi M, Herndon DN, Suzuki F. CCL17 and IL-10 as effectors that enable alternatively activated macrophages to inhibit the generation of classically activated macrophages. *J Immunol* 2004;172:1407-1413.

(20) Bhan U, Lukacs NW, Osterholzer JJ, Newsteas MW, Zeng X, Moore TA, McMillan TR, Krieg AM, Akira S, Standiford TJ. TLR9 is required for protective innate immunity in Gram-negative bacterial pneumonia: role of dendritic cells. *J Immunol* 2007;179:3937-3946.

(21) Akira S, Uematsu S, Takeuchi O. Pathogen recognition and innate immunity. *Cell* 2006;124;783-801.

(22) Trinchieri G, Sher A. Cooperation of Toll-like receptor signals in innate immune defense. *Nat Rev Immunol* 2007;7:179-190.

(23) Xu D, Liu H, Komai-Koma M. Direct and indirect role of Toll-like receptors in T cell mediated immunity. *Cell Mol Immunol* 2004;1:239–246.

(24) Pasare C, Medzhitov R. Toll-like receptors: linking innate and adaptive

immunity. *Adv Exp Med Biol* 2005;560:11–18.

(25) Gon Y. Toll-like receptors and airway inflammation. *Allergol Int* 2008;57:33-37.

(26) John G, Yildirim AO, Rubin BK, Gruenert DC, Henke MO. Toll-like Receptor (TLR)-4 Mediated Innate Immunity is Reduced in Cystic Fibrosis Airway Cells. *Am J Respir Cell Mol Biol*. (In press)

(27) Blohmke CJ, Victor RE, Hirschfeld AF, Elias IM, Hancock DG, Lane CR, Davidson AG, Wilcox PG, Smith KD, Overhage J, Hancock RE, Turvey SE. Innate immunity mediated by TLR5 as a novel antiinflammatory target for cystic fibrosis lung disease. *J Immunol* 2008;180:7764-7773.

(28) Kato A, Favoreto S Jr, Avila PC, Schleimer RP. TLR3- and Th2 cytokine-dependent production of thymic stromal lymphopoietin in human airway epithelial cells. *J Immunol* 2007;179:1080-1087.

(29) Kane CM, Cervi L, Sun J, McKee AS, Masek KS, Shapira S, Hunter CA, Pearce EJ. Helminth antigens modulate TLR-initiated dendritic cell activation. *J Immunol* 2004;173:7454-7461.

(30) Pearce EJ. Priming of the immune response by schistosome eggs. *Parasite Immunol* 2005;27:265-270.

(31) Gordon S. Alternative activation of macrophages. *Nat Rev Immunol* 2003;3:23-35.

(32) Liu T, Jin H, Ullenbruch M, Hu B, Hashimoto N, Moore B, McKenzie A, Lukacs NW, Phan SH. Regulation of found in inflammatory zone 1 expression in bleomycin-induced lung fibrosis: role of IL-4/IL-13 and mediation via STAT-6. *J Immunol* 2004;173:3425-3431.

(33) Munder M, Eichmann K, Modolell M. Alternative metabolic states in murine macrophages reflected by the nitric oxide synthase/arginase balance: competitive regulation by $CD4^+$ T cells correlates with Th1/Th2 phenotype. *J Immunol* 1998;160:5347-5354.

(34) Liu T, Dhanasekaran SM, Jin H, Hu B, Tomlins SA, Chinnaiyan AM, Phan SH. FIZZ1 stimulation of myofibroblast differentiation. *Am J Pathol* 2004;164:1315-1326.

(35) Chung, MJ, Liu T, Ullenbruch M, Phan SH. Antiapoptotic effect of found in inflammatory zone (FIZZ)1 on mouse lung fibroblasts. *J Pathol* 2007;212:180-187.

(36) Angelini DJ, Su Q, Yamaji-Kegan K, Fan C, Skinner JT, Champion HC, Crow MT, Johns RA. Hypoxia-induced mitogenic factor (HIMF/FIZZ1/RELMalpha) induces the vascular and hemodynamic changes of pulmonary hypertension. *Am J Physiol Lung Cell Mol Physiol* 2009;296:L582-L593.

(37) Phan SH. Biology of fibroblasts and myofibroblasts. Proc Am Thorac Soc 2008;5:334-337.

(38) Petrov VV, Fagard RH, Lijnen PJ. Stimulation of collagen production by transforming growth factor-beta1 during differentiation of cardiac fibroblasts to myofibroblasts. *Hypertension* 2002;39:258–263.

(39) Kolodsick JE, Toews GB, Jakubzick C, Hogaboam C, Moore TA, McKenzie A, Wilke CA, Chrisman CJ, Moore BB. Protection from fluorescein isothiocyanate-induced fibrosis in IL-13-deficient, but not IL-4-deficient, mice results from impaired collagen synthesis by fibroblasts. J Immunol 2004;172:4068-4076.

(40) Wynn TA. Cellular and molecular mechanisms of fibrosis. *J Pathol* 2008;214:199-210.

(41) Yoshie O, Imai T, Nomiyama H. Chemokines in immunity. *Adv Immunol* 2001;78:57-110.

(42) Martinez FO, Sica A, Mantovani A, Locati M. Macrophage activation and polarization. *Front Biosci* 2008;13:453-61.

Figure legends

Figure 1. TLR9$^{-/-}$ mice showed larger pulmonary granulomas and enhanced collagen deposition. All panels compare parameters between WT and TLR9$^{-/-}$ mice. (*A*) Lung tissues were histologically analyzed by Masson's Trichrome staining at day 4, 8, 16, and 30 after initiation of lung granuloma. Original magnification, x40 or x400. (*B*) Kinetic analysis of the development of lung granulomas using morphometric analysis of the evolving lung lesions in WT and TLR9$^{-/-}$ mice. Dotted line represents mean granuloma cross-sectional area (μm^2) ± SEM. *$P < 0.05$; **$P < 0.001$. (*C*) The percentage of collagen in each granuloma was quantified using IP lab software. *$P < 0.05$; **$P < 0.01$. (*D*) Quantitative real-time PCR (TaqMan) was performed to measure the transcript level of α-SMA in whole lungs. *$P < 0.05$; **$P < 0.01$. (*E*) Confocal immunofluorescent examination of pulmonary granulomas showed increased α-SMA$^+$ cells (green) in TLR9$^{-/-}$ mice. Shown are representative sections from 1 mouse of 4 per group. Original magnification, x400. For Fig 1A-Fig 1D, data shown are mean ± SEM and are from a representative example of 3 independent experiments. n= 4-5 mice per group.

Figure 2. TLR9$^{-/-}$ mice showed impaired Th1 cytokine and enhanced Th2 cytokine levels. All panels compare parameters between WT and TLR9$^{-/-}$ mice. (*A*) Protein levels of IFN-γ, IL-12(p70), TNF-α, IL-4, IL-5, and IL-13 measured in whole lungs using a luminex system. Data shown are mean ± SEM and are from a representative example of 3 independent experiments. Each time point indicates at least 4–5 mice per group. *$P < 0.05$; **$P < 0.01$. (*B*) Whole cells from the draining lymph nodes of WT or TLR9$^{-/-}$ mice at days 16 after *S. mansoni* egg challenge were re-stimulated *in vitro* with SEA for 48 h.

Cytokine levels of IFN-γ, IL-4, IL-5, and IL-13 were measured using a luminex system. *$P < 0.05$. Data shown are mean ± SEM and are from a representative example of 3 independent experiments.

Figure 3. TLR9$^{-/-}$ mice showed decreased M1 markers and increased M2 markers during *S. mansoni* egg challenge. All panels compare parameters between WT and TLR9$^{-/-}$ mice. The gene expression level of FIZZ1 (*A*), Arginase-1 (*C*) and iNOS (*D*), and the protein level of FIZZ1 (*B*) in the whole lungs at days 0, 4, 8, 16, 30 are shown. *$P < 0.05$; **$P < 0.01$. Data shown are mean ± SEM and are from a representative example of 3 independent experiments. n= 4-5 mice per group.

Figure 4. Impaired migration of DCs in TLR9$^{-/-}$ mice during pulmonary granuloma formation. FACS analysis of lung DCs (*A*) and macrophages (*B*) isolated from *S. mansoni* egg challenged mice. *$P < 0.05$ compared with WT mice. (*C*) Confocal immunofluorescent examination of pulmonary granulomas showed fewer CD11c^{+} cells (red arrow) and increased F4/80^{+} cells (green arrow) in TLR9$^{-/-}$ mice. Shown are representative sections from 1 mouse of 4 per group. Original magnification, ×400. (*D*) Quantitative real-time PCR (TaqMan) was performed to measure the transcript levels of chemokines in whole lungs at day 16 after the initiation of lung granuloma. *$P < 0.05$; **$P < 0.01$. Data shown indicate mean ± SEM and are from a representative example of 3 independent experiments. n= 4 mice per group.

Figure 5. BM-derived DCs but not BM-derived macrophages promote the differentiation

of Th1 and Th2 cells from T cells re-stimulated with SEA. $CD4^+$ T cells were isolated from spleens of *S. mansoni* egg-challenged WT mice and re-stimulated with DCs or macrophages isolated from WT or $TLR9^{-/-}$ mice, as indicated. Cytokine levels of IFN-γ (*A*), IL-4 (*B*), IL-5 (*C*), and IL-13 (*D*) were measured using a luminex system. $^*P < 0.05$. Data shown indicate mean ± SEM and are from a representative example of 3 independent experiments. n= 4 mice per group. MØ = Macrophage

Figure 6. BM-derived DCs from *S. mansoni* egg-challenged mice promoted an enhanced Th2 response. $CD4^+$ T cells were isolated from lungs of *S. mansoni* egg-challenged WT mice and re-stimulated with DCs or macrophages isolated from naïve or SEA stimulated WT or $TLR9^{-/-}$ mice, as indicated. Cytokine levels of IFN-γ (*A*), IL-4 (*B*), IL-5 (*C*), and IL-13 (*D*) were measured using a luminex system. $^*P < 0.05$ compared with naïve DC, and $^{\#}P < 0.05$ compared with WT mice. Data shown indicate mean ± SEM and are from a representative example of 3 independent experiments. n= 4 mice per group.

Figure 7. Effect of i.t. administration of BM-derived DC from either WT or $TLR9^{-/-}$ mice on granuloma formation in $TLR9^{-/-}$ mice with *S. mansoni* egg. (*A*) Histological appearance of pulmonary granulomas from $TLR9^{-/-}$ mice treated with either PBS, WT-DC or $TLR9^{-/-}$-DC at day 16 after granuloma development. Arrows point out collagen deposition. H&E staining and Masson's Trichrome staining. Original magnification, x40; x400. Experiments were performed 3 times with similar results. (*B*) Morphometric analysis of pulmonary granuloma size from mice treated with either PBS, WT-DC or $TLR9^{-/-}$-DC after 16 days of lung granuloma development. $^{**}P < 0.01$. (*C*) The

percentage of collagen in each granuloma was quantified using IP lab software. $^{**}P < 0.01$. Data shown indicate mean ± SEM and are from a representative example of 2 independent experiments. n= 4-5 mice per group. TR = Masson's Trichrome staining.

Figure 8. The intratracheal delivery of WT-DC into TLR9$^{-/-}$ mice resulted in a marked reduction in Th2 cytokines and M2 phenotype. (*A*-*D*) Protein level of IL-4 (*A*), IL-5 (*B*), IL-13 (*C*) and FIZZ1 (*D*) was measured in whole lungs using a Luminex system or ELISA system. $^{*}P < 0.05$; $^{**}P < 0.01$. Data shown indicate mean ± SEM and are from a representative example of 2 independent experiments. n= 4-5 mice per group.

Figure 9. Recombinant FIZZ1 administration during granuloma formation induced enhanced collagen deposition. (*A*) Lung tissues were histologically analyzed by H&E and Masson's Trichrome staining at day 16 after initiation of lung granuloma. Arrows point out collagen deposition. Original magnification, x400. (*B*) The percentage of collagen in each granuloma was quantified using IP lab software. $^{*}P < 0.05$; $^{**}P < 0.01$. Data shown indicate mean ± SEM and are from a representative example of 2 independent experiments. n= 5 mice per group. rFIZZ1 = recombinant FIZZ1.

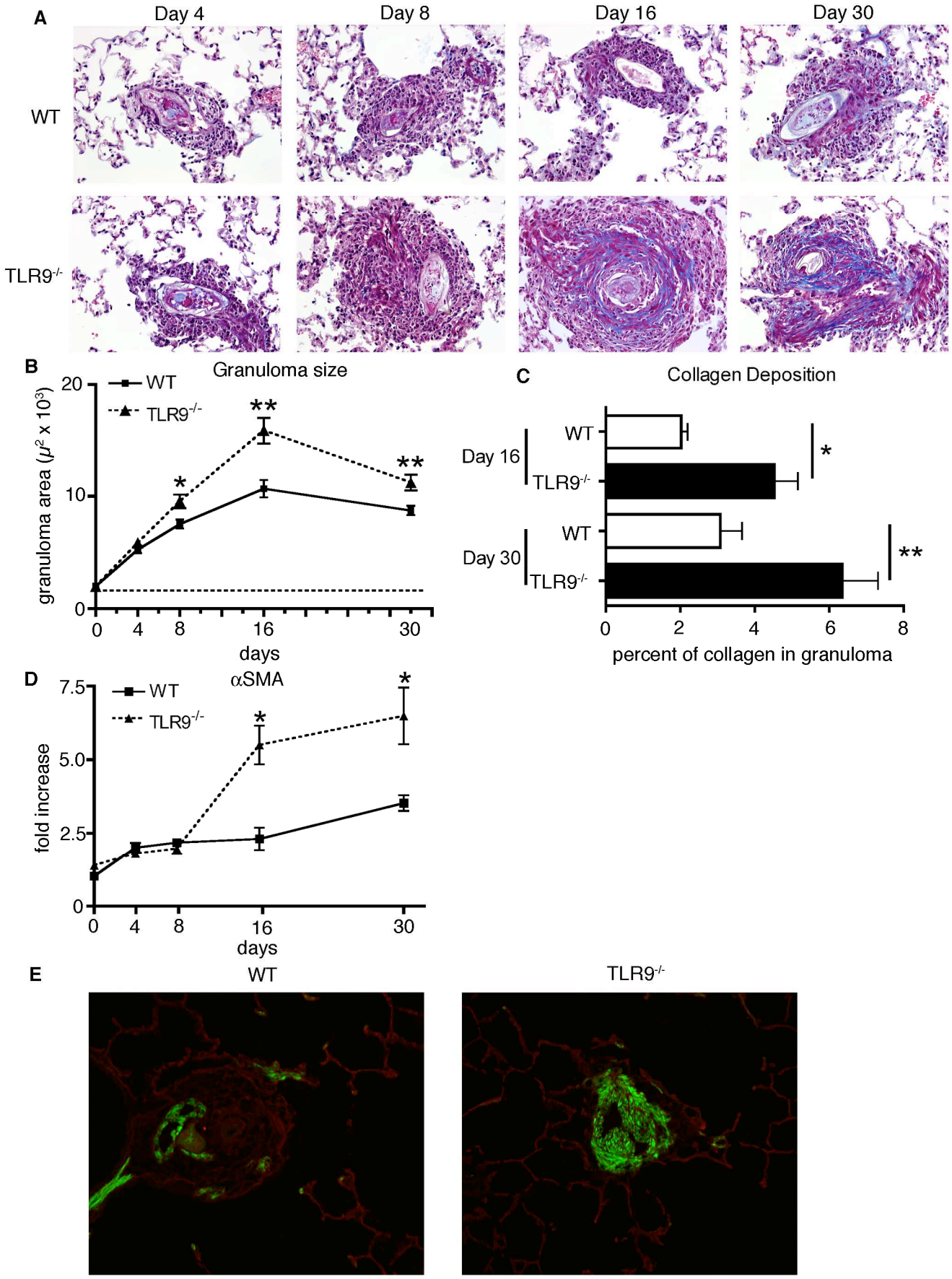
A
Day 4
Day 8
Day 16
Day 30
WT
TLR9-/-
B
Granuloma size
WT
TLR9-/-
granuloma area (μ2 x 10³)
20
10
0
0
4
8
16
30
days
*
**
**
C
Collagen Deposition
Day 16
Day 30
WT
TLR9-/-
WT
TLR9-/-
*
**
0
2
4
6
8
percent of collagen in granuloma
D
αSMA
WT
TLR9-/-
fold increase
7.5
5.0
2.5
0
0
4
8
16
30
days
*
*
E
WT
TLR9-/-

Figure 1

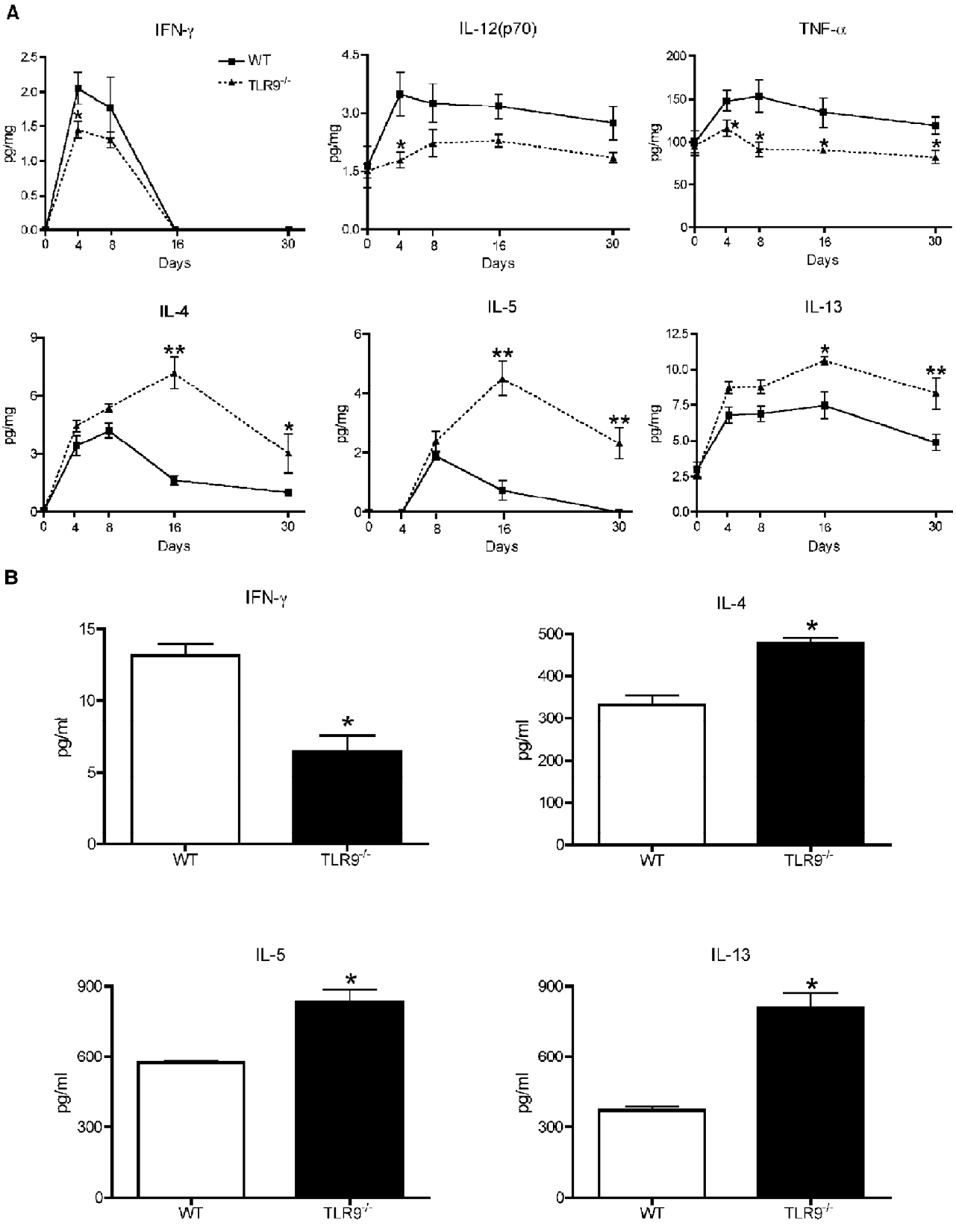
A
IFN-γ
IL-12(p70)
TNF-α
WT
TLR9-/-
pg/mg
Days
IL-4
IL-5
IL-13
B
IFN-γ
IL-4
IL-5
IL-13
pg/ml
WT
TLR9-/-

Figure 2

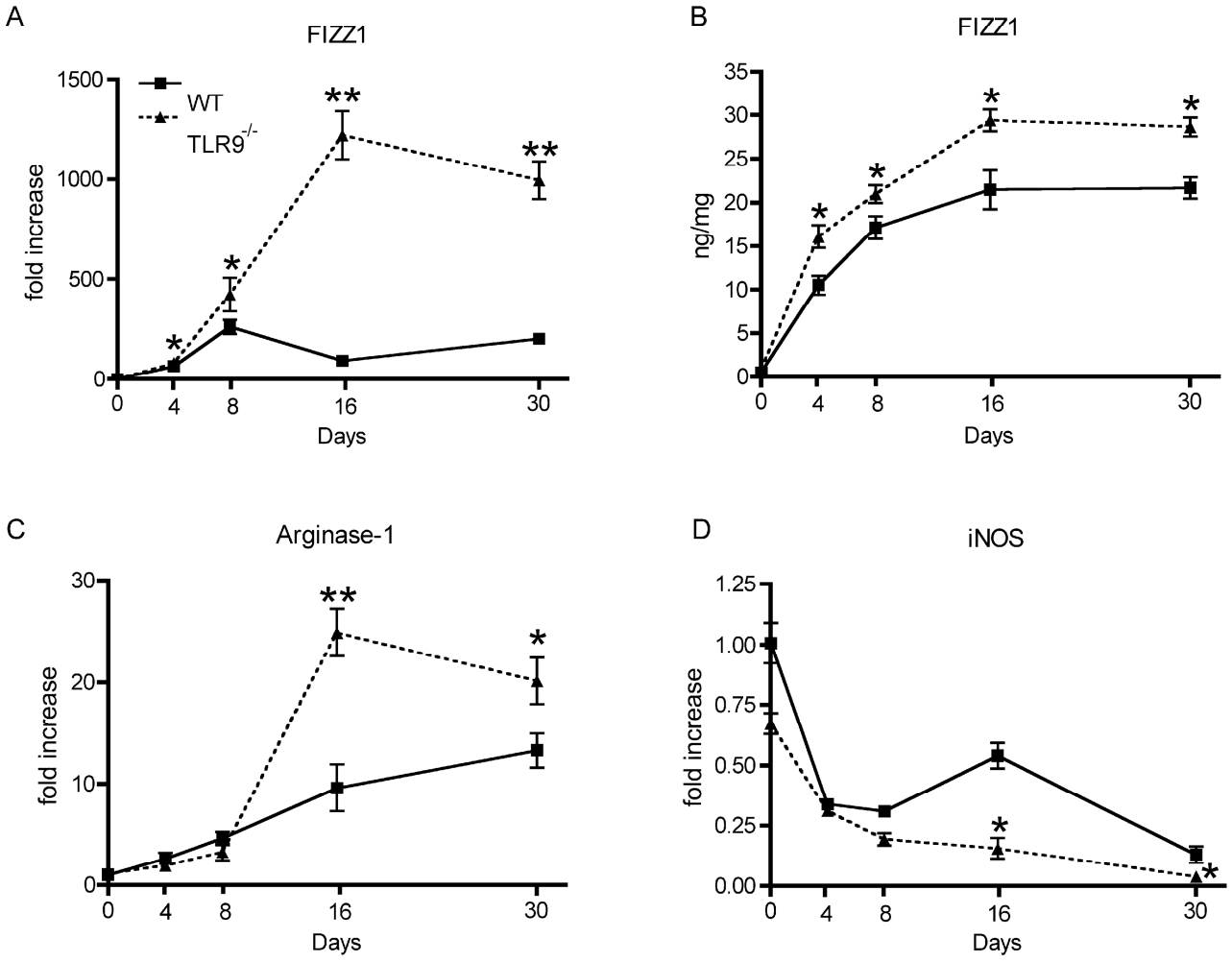
A
FIZZ1
WT
TLR9-/-
fold increase
1500
1000
500
0
0
4
8
16
30
Days
B
FIZZ1
ng/mg
35
30
25
20
15
10
5
0
Days
C
Arginase-1
fold increase
30
20
10
0
Days
D
iNOS
fold increase
1.25
1.00
0.75
0.50
0.25
0.00
Days

Figure 3

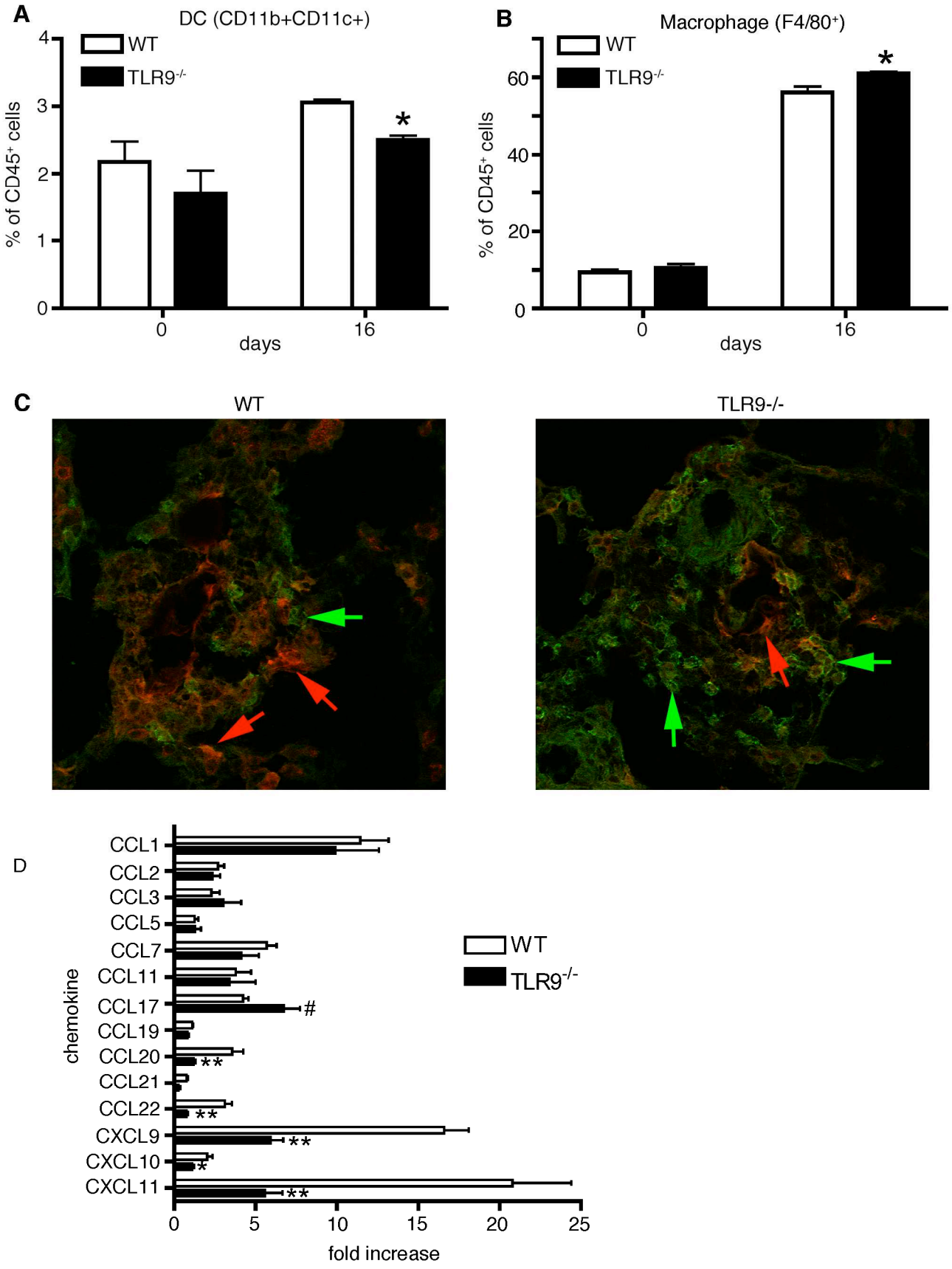
A
DC (CD11b+CD11c+)
WT
TLR9-/-
% of CD45+ cells
0
1
2
3
4
0
16
days
*
B
Macrophage (F4/80+)
WT
TLR9-/-
% of CD45+ cells
0
20
40
60
0
16
days
*
C
WT
TLR9-/-
D
chemokine
CCL1
CCL2
CCL3
CCL5
CCL7
CCL11
CCL17
CCL19
CCL20
CCL21
CCL22
CXCL9
CXCL10
CXCL11
#
**
**
**
*
**
WT
TLR9-/-
0
5
10
15
20
25
fold increase

Figure 4

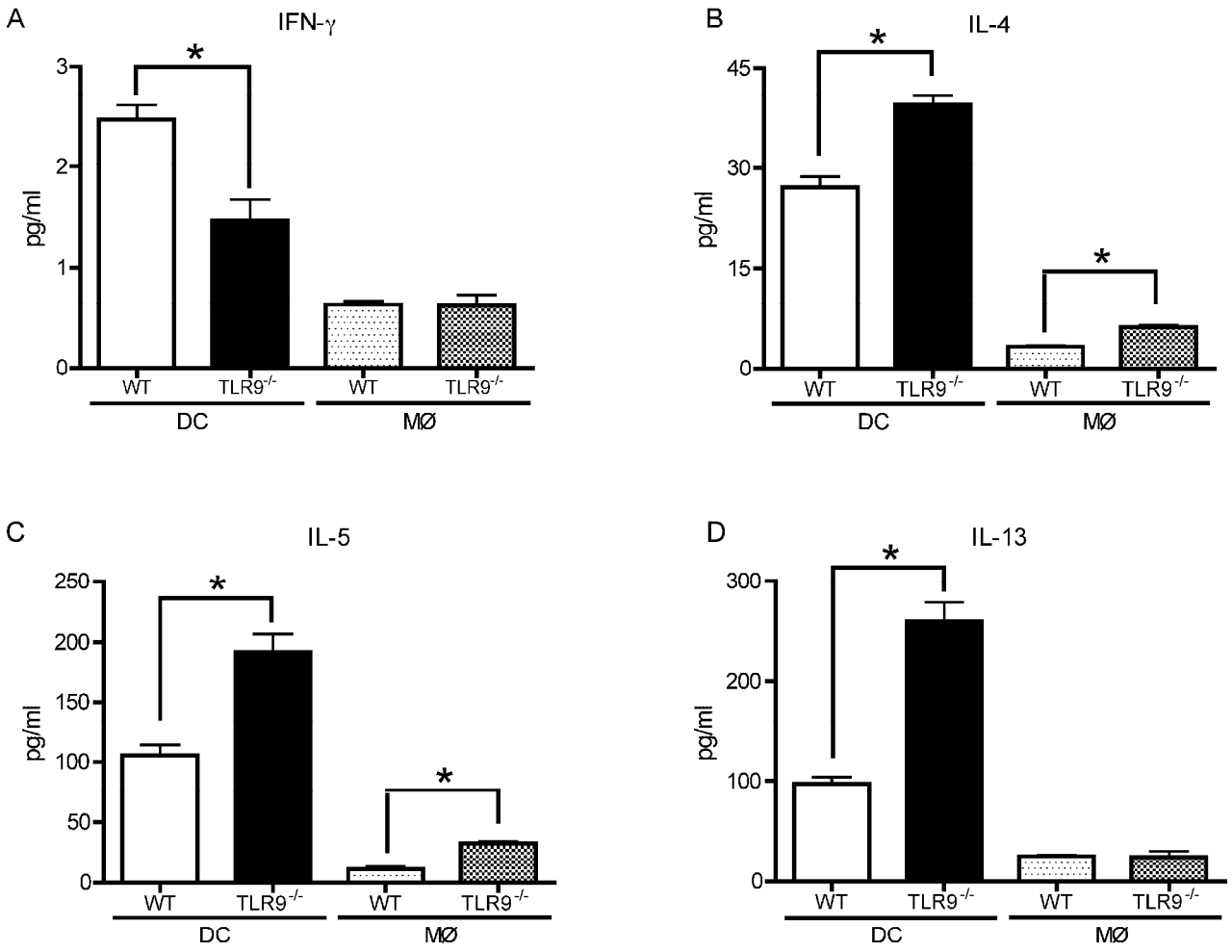
A
IFN-γ
pg/ml
3
2
1
0
*
WT
TLR9-/-
WT
TLR9-/-
DC
MØ
B
IL-4
pg/ml
45
30
15
0
*
*
WT
TLR9-/-
WT
TLR9-/-
DC
MØ
C
IL-5
pg/ml
250
200
150
100
50
0
*
*
WT
TLR9-/-
WT
TLR9-/-
DC
MØ
D
IL-13
pg/ml
300
200
100
0
*
WT
TLR9-/-
WT
TLR9-/-
DC
MØ

Figure 5

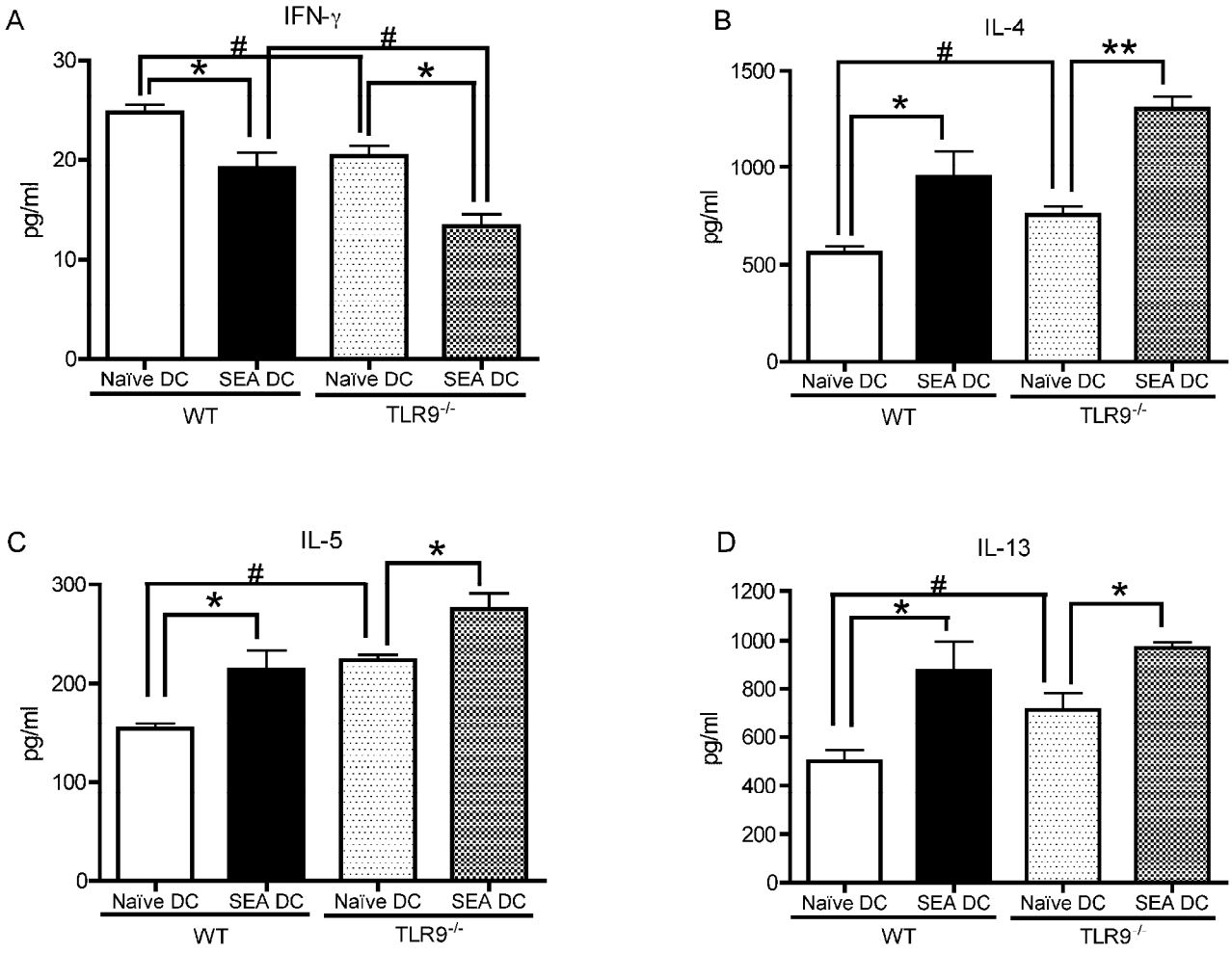
A
IFN-γ
pg/ml
30
20
10
0
#
#
*
*
Naïve DC
SEA DC
Naïve DC
SEA DC
WT
TLR9-/-
B
IL-4
pg/ml
1500
1000
500
0
#
**
*
Naïve DC
SEA DC
Naïve DC
SEA DC
WT
TLR9-/-
C
IL-5
pg/ml
300
200
100
0
#
*
*
Naïve DC
SEA DC
Naïve DC
SEA DC
WT
TLR9-/-
D
IL-13
pg/ml
1200
1000
800
600
400
200
0
#
*
*
Naïve DC
SEA DC
Naïve DC
SEA DC
WT
TLR9-/-

Figure 6

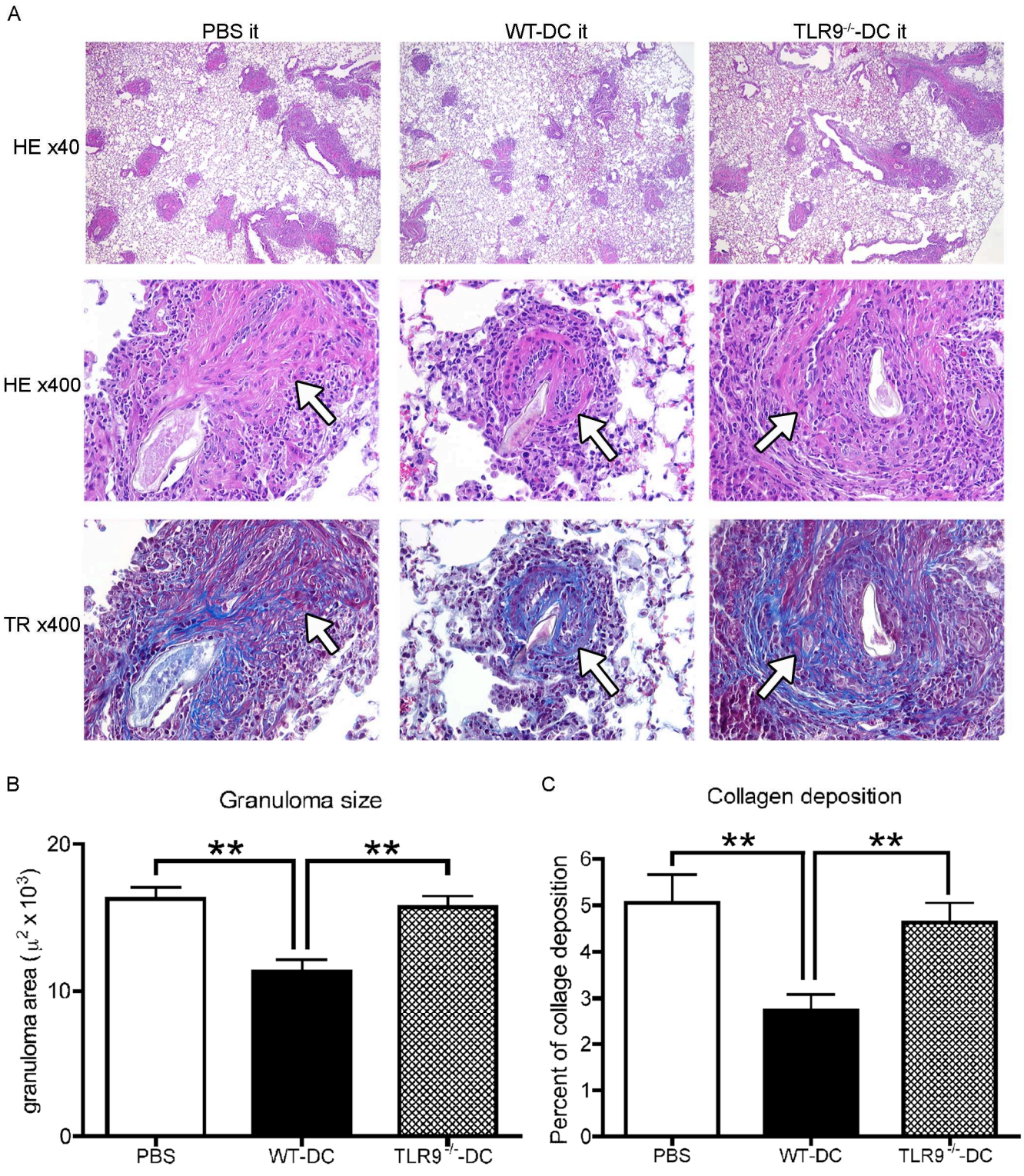
A
PBS it
WT-DC it
TLR9-/--DC it
HE x40
HE x400
TR x400
B
Granuloma size
granuloma area (μ2 x 10³)
20
10
0
**
**
PBS
WT-DC
TLR9-/--DC
C
Collagen deposition
Percent of collage deposition
6
5
4
3
2
1
0
**
**
PBS
WT-DC
TLR9-/--DC

Figure 7

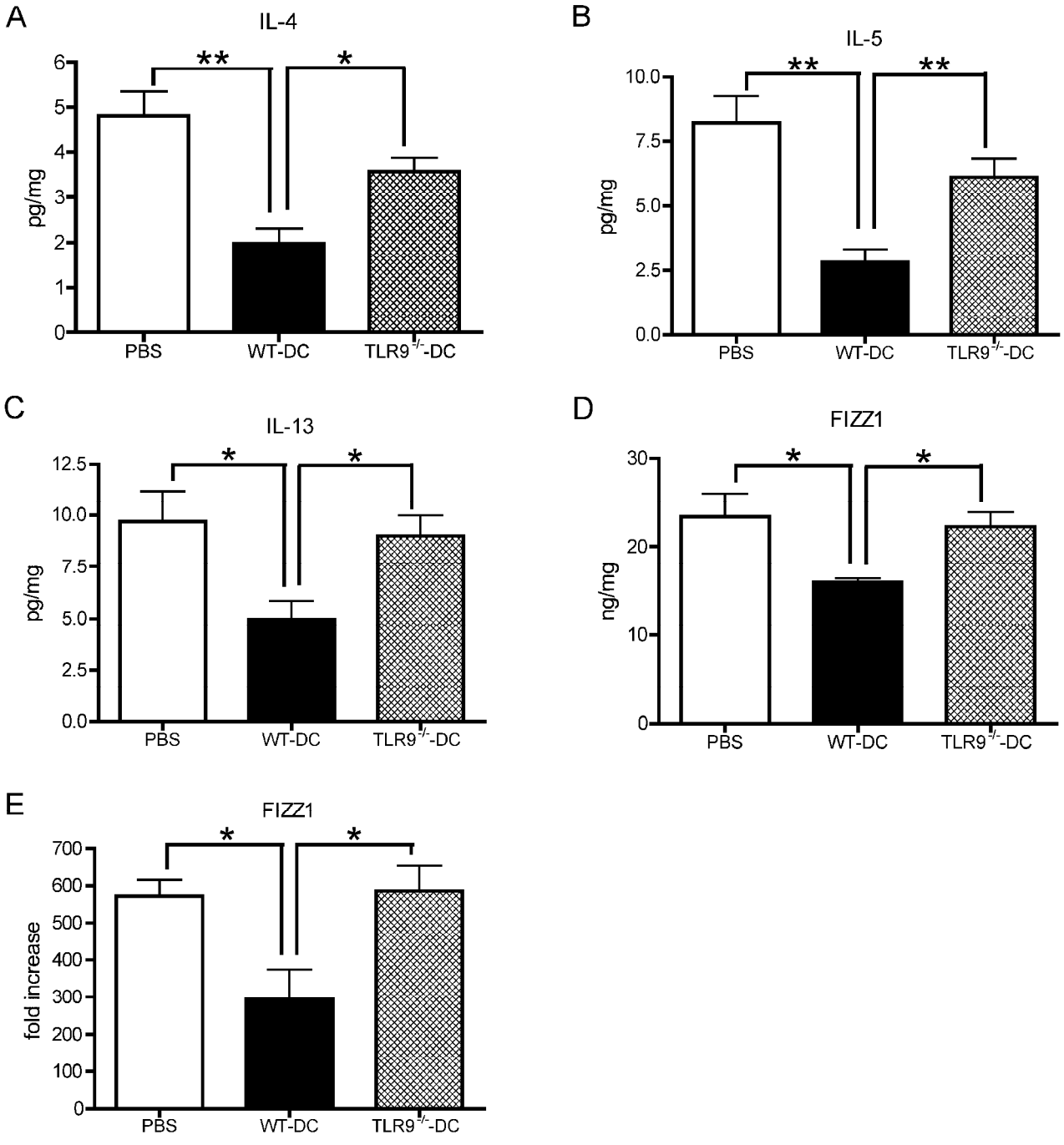
A
IL-4
pg/mg
6
5
4
3
2
1
0
**
*
PBS
WT-DC
TLR9-/--DC
B
IL-5
pg/mg
10.0
7.5
5.0
2.5
0.0
**
**
PBS
WT-DC
TLR9-/--DC
C
IL-13
pg/mg
12.5
10.0
7.5
5.0
2.5
0.0
*
*
PBS
WT-DC
TLR9-/--DC
D
FIZZ1
ng/mg
30
20
10
0
*
*
PBS
WT-DC
TLR9-/--DC
E
FIZZ1
fold increase
700
600
500
400
300
200
100
0
*
*
PBS
WT-DC
TLR9-/--DC

Figure 8

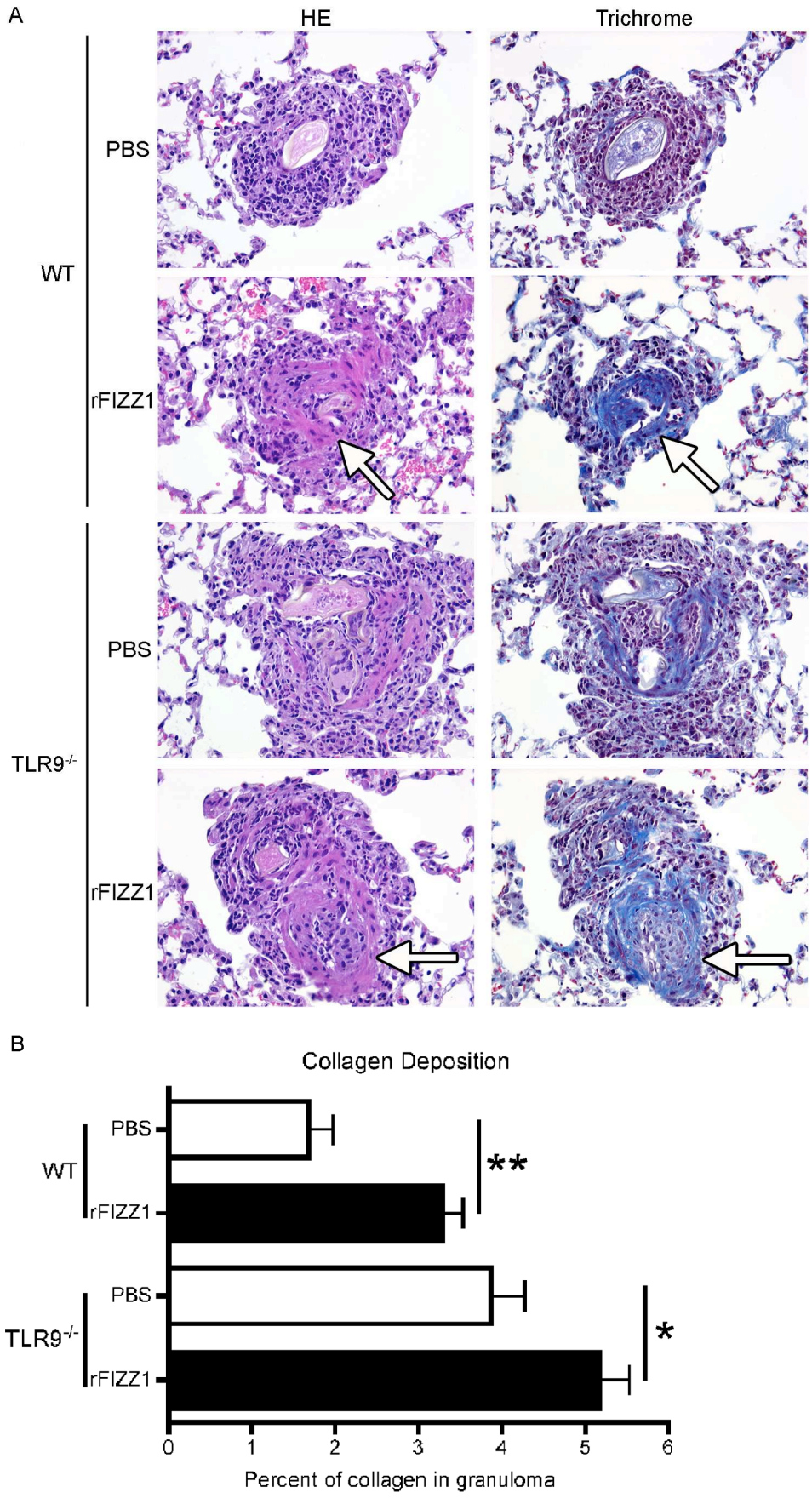
A
HE
Trichrome
PBS
WT
rFIZZ1
PBS
TLR9-/-
rFIZZ1
B
Collagen Deposition
PBS
WT
rFIZZ1
**
PBS
TLR9-/-
rFIZZ1
*
0
1
2
3
4
5
6
Percent of collagen in granuloma

Figure 9

Toll-like Receptor 9 Activation is a Key Mechanism for the Maintenance of Chronic Lung Inflammation

Toshihiro Ito, Matthew Schaller, Tracy Raymond, Amrita D. Joshi, Ana L. Coelho, Fabiani G. Frantz, William F. Carson IV, Cory M. Hogaboam, Nicholas W. Lukacs, Theodore J. Standiford, Sem H. Phan, Stephen W. Chensue, and Steven L. Kunkel

ONLINE DATA SUPPLEMENT

Supplemental Figure 1. TLR9$^{-/-}$ mice showed impaired Th1-related cytokine levels during granuloma development. Quantitative real-time PCR (TaqMan) was performed to measure the transcript levels of IFN-γ (*A*), IL-12(p35) (*B*), and TNF-α (*C*) in whole lungs. *$P < 0.05$ compared with WT mice. Data shown are mean ± SEM and are from a representative example of 3 independent experiments. n= 4-5 mice per group.

Supplemental Figure 2. BM-derived DCs from *S. mansoni* egg-challenged mice promoted enhanced Th2 response. CD4$^+$ T cells were isolated from draining lymph nodes of *S. mansoni* egg-challenged WT mice and re-stimulated with DCs or macrophages isolated from WT or TLR9$^{-/-}$ mice, as indicated. Cytokine levels of IFN-γ (*A*), IL-4 (*B*), IL-5 (*C*), and IL-13 (*D*) were measured using a luminex system. *$P < 0.05$ compared with naïve DC, and $^{\#}P < 0.05$ compared with WT mice. Data shown indicate mean ± SEM and are from a representative example of 2 independent experiments. n= 4 mice per group.

Supplemental Figure 3. No significant differences in cytokine production in T cells co-cultured with BM-derived DCs from WT or TLR9$^{-/-}$ mice after stimulation with OVA. Splenic CD4$^+$ T cells were isolated from DO11.10 mice and stimulated with OVA-pulsed BM-derived DCs from either WT or TLR9$^{-/-}$ mice. (*A*) IFN-γ production. (*B*) IL-4 production. (*C*) IL-5 production. (*D*) IL-13 production. Data shown indicate mean ± SEM and are from a representative example of 2 independent experiments. n= 4 mice per group.

Supplemental Figure 4. Effect of i.t. administration of BM-derived DC from either WT or TLR9$^{-/-}$ mice on granuloma formation in TLR9$^{-/-}$ mice. Whole cells from the draining lymph nodes of TLR9$^{-/-}$ mice treated with either PBS, WT-DC or TLR9$^{-/-}$-DC after 16 days of lung granuloma development were re-stimulated *in vitro* with SEA for 48 h. Cytokine levels of IFN-γ (*A*), IL-4 (*B*), IL-5 (*C*), and IL-13 (*D*) were measured using a luminex system. *$P < 0.05$. Data shown are mean ± SEM and are from a representative example of 2 independent experiments. n= 4-5 mice per group.

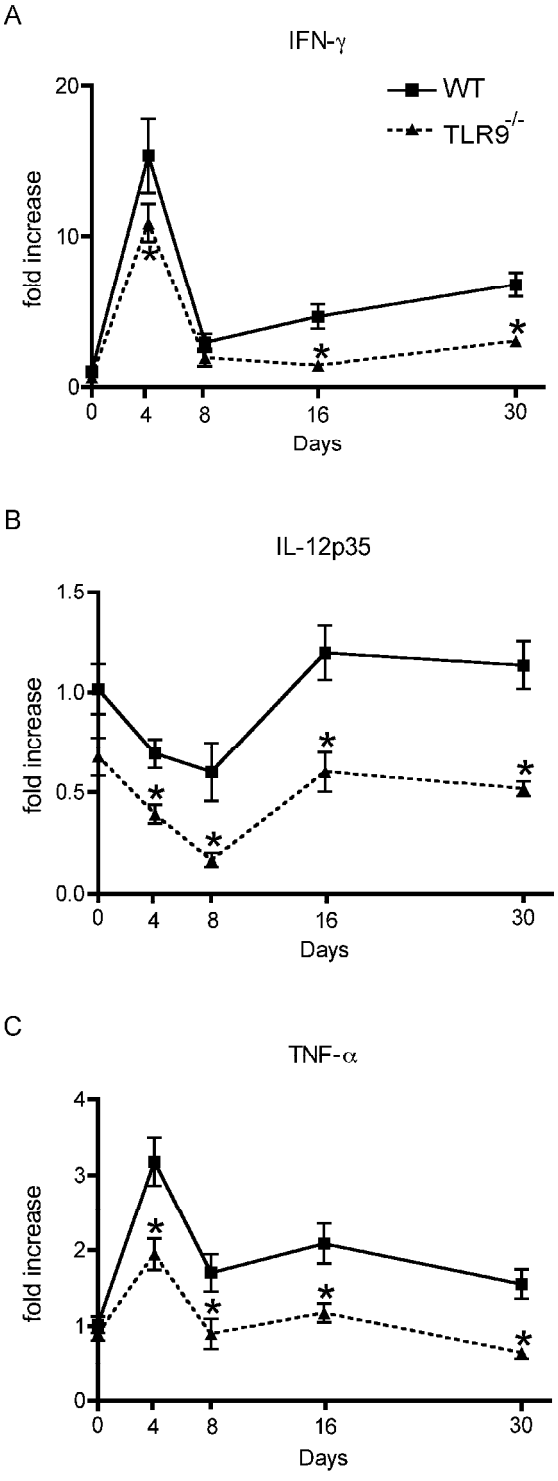
A
IFN-γ
WT
TLR9-/-
fold increase
20
10
0
0
4
8
16
30
Days
B
IL-12p35
fold increase
1.5
1.0
0.5
0.0
0
4
8
16
30
Days
C
TNF-α
fold increase
4
3
2
1
0
0
4
8
16
30
Days

Figure E1

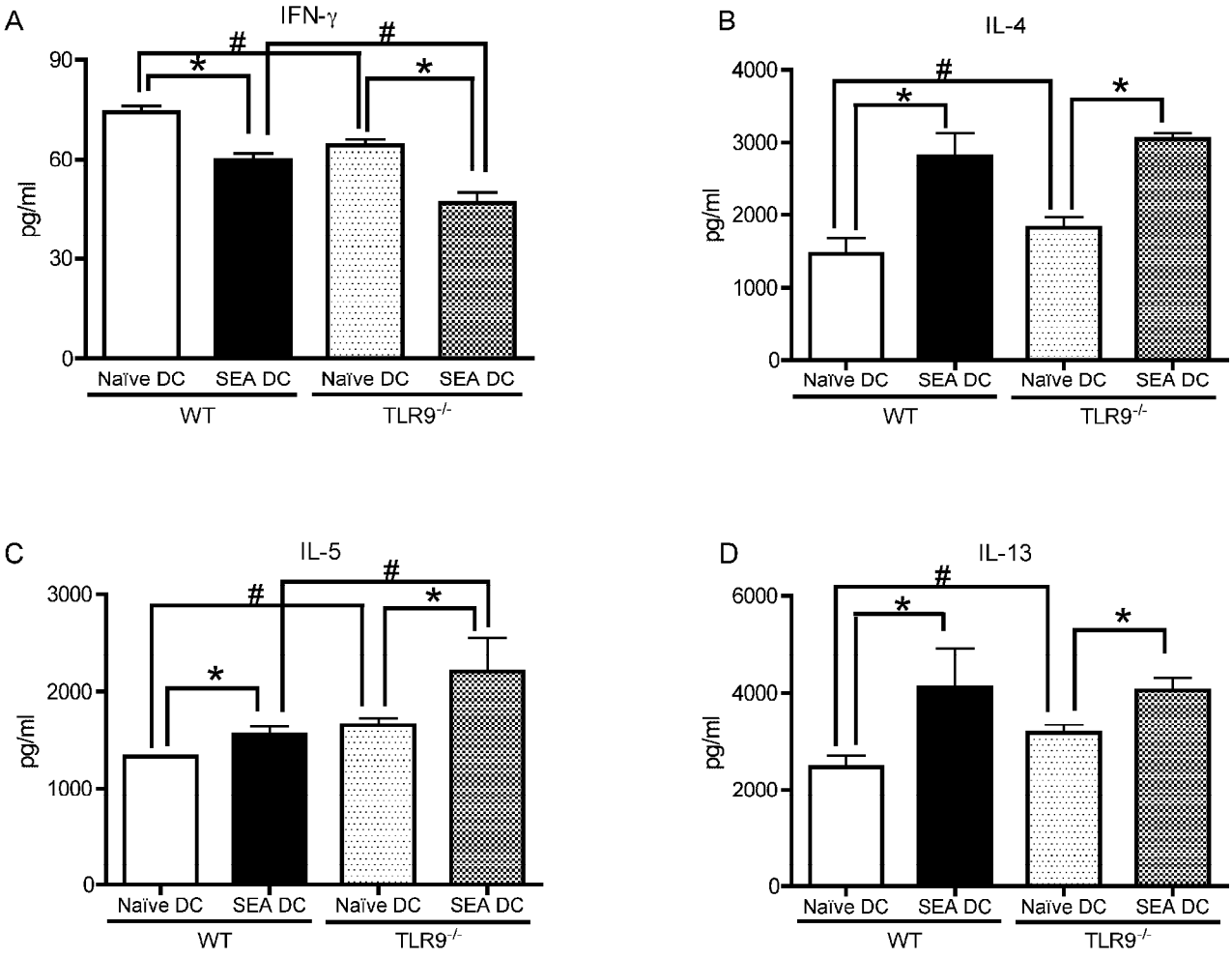
A
IFN-γ
pg/ml
90
60
30
0
#
#
*
*
Naïve DC
SEA DC
Naïve DC
SEA DC
WT
TLR9-/-
B
IL-4
pg/ml
4000
3000
2000
1000
0
#
*
*
Naïve DC
SEA DC
Naïve DC
SEA DC
WT
TLR9-/-
C
IL-5
pg/ml
3000
2000
1000
0
#
#
*
*
Naïve DC
SEA DC
Naïve DC
SEA DC
WT
TLR9-/-
D
IL-13
pg/ml
6000
4000
2000
0
#
*
*
Naïve DC
SEA DC
Naïve DC
SEA DC
WT
TLR9-/-

Figure E2

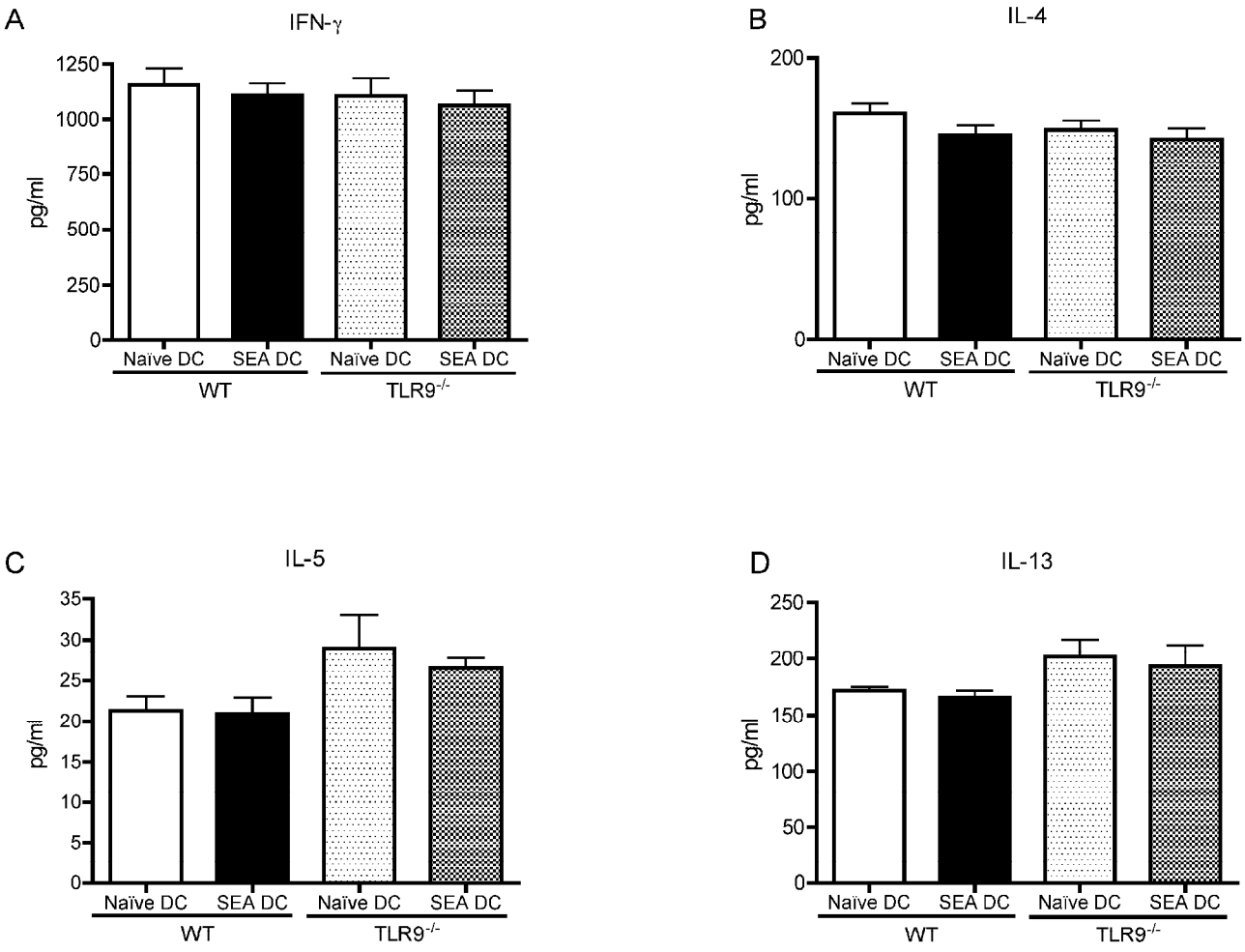
A
IFN-γ
pg/ml
1250
1000
750
500
250
0
Naïve DC
SEA DC
Naïve DC
SEA DC
WT
TLR9-/-
B
IL-4
pg/ml
200
100
0
Naïve DC
SEA DC
Naïve DC
SEA DC
WT
TLR9-/-
C
IL-5
pg/ml
35
30
25
20
15
10
5
0
Naïve DC
SEA DC
Naïve DC
SEA DC
WT
TLR9-/-
D
IL-13
pg/ml
250
200
150
100
50
0
Naïve DC
SEA DC
Naïve DC
SEA DC
WT
TLR9-/-

Figure E3

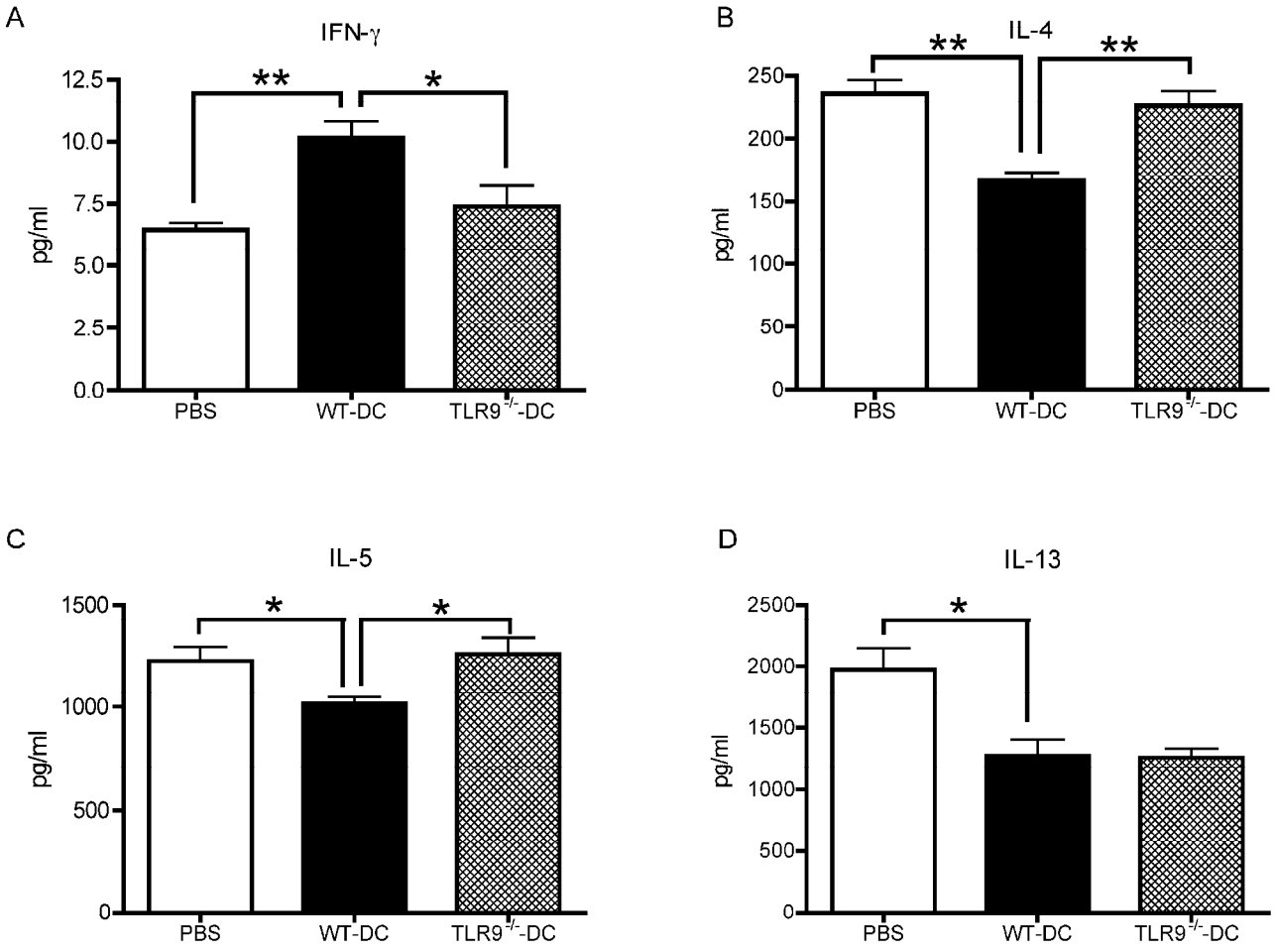
A
IFN-γ
pg/ml
12.5
10.0
7.5
5.0
2.5
0.0
**
*
PBS
WT-DC
TLR9-/--DC
B
IL-4
pg/ml
250
200
150
100
50
0
**
**
PBS
WT-DC
TLR9-/--DC
C
IL-5
pg/ml
1500
1000
500
0
*
*
PBS
WT-DC
TLR9-/--DC
D
IL-13
pg/ml
2500
2000
1500
1000
500
0
*
PBS
WT-DC
TLR9-/--DC

Figure E4